J Mater Sci (2007) 42:4535–4544
DOI 10.1007/s10853-006-0476-y

Some aspects of corrosion and film formation of austenitic stainless steel type 316LN using electrochemical impedance spectroscopy (EIS)

Mohan G. Pujar · N. Parvathavarthini · R. K. Dayal

Received: 6 August 2005 / Accepted: 31 May 2006 / Published online: 15 February 2007

Abstract Corrosion and passive film characteristics of 316LN stainless steel with different degrees of cold work (0–25%) were studied using electrochemical impedance spectroscopy (EIS) and potentiodynamic anodic polarization techniques in deaerated acidic and alkaline (pH = 8) media. EIS measurements were conducted at open circuit potential (OCP) as well as after passivation in these media. Using the capacitance data from EIS measurements, film thickness was calculated. A definite correlation was observed between film thickness and corrosion rate after passivation. Analysis of the series capacitance and series resistance data from the EIS spectra showed that the films formed at OCP and after passivation were of semiconducting type. The nature of the semiconducting type of films was determined to be *n*-type using the ratios of anodic and cathodic transfer coefficients (α_a/α_c).

Introduction

It is known that the nature of passive films on metals and alloys is the ultimate factor, which controls their corrosion behaviour. Various theories have been put forth to explain the passivation processes and are classified as: (1) metal modification theories, (2) rate velocity theories, (3) oxide film theories, and (4) adsorption theories. Currently the most widely accepted theories belong to the last two categories. The passive films formed have a profound influence on the electrooxidative process of stainless steel. The structure and composition of the film formed may depend on a large number of variables like, pretreatment, composition of the metal surface, the electrode potential, the polarization time, the environment chemistry, temperature etc [1]. Bianchi et al. [2] interpreted the electrochemical behaviour of the passive films on the stainless steels in terms of the semiconducting properties of the films and relationships were formulated between the conductivity type and the protecting efficiency of the passive films. Passive films grown on alloys are not homogeneous both at macro as well as at microscopic scale and are most frequently non-stoichiometric oxides of amorphous or polycrystalline structure [3, 4]. As the presence of a semiconducting oxide film determines the charge distribution and the potential drop at the metal-metal oxide-electrolyte interface, capacitive studies of this system can yield significant information not only about the film formation process but also about the electronic structure of the film [5]. For these reasons in recent years much work has been devoted to the study of the chemico-physical properties of passive layers on metals and alloys. Though, several references give details about the capacitance measurements on passive iron [6–10], only a few papers reported such measurements for passive stainless steels [11–13]. The earlier capacitance measurements dealt with the kinetics

M. G. Pujar (✉) · N. Parvathavarthini · R. K. Dayal
Corrosion Science & Technology Section–Reactor Materials (CSTS–RM), Indira Gandhi Centre for Atomic Research, Kalpakkam, TN 603 102, India
e-mail: mgpujar@yahoo.co.in

N. Parvathavarthini
e-mail: npv@igcar.gov.in

R. K. Dayal
e-mail: rkd@igcar.gov.in

of the film growth on austenitic stainless steels in both pitting and non-pitting environments. But most of the data was generated at only one frequency. Although some work has been reported on the electrochemical behaviour of stainless steels in acidic, neutral and alkaline solutions, still a clear picture on the electronic structure of passive layers has not been well established. In the present work, EIS technique was employed in order to study capacitance behaviour of austenitic stainless steel of type 316LN with 0–25% cold work in deaerated acidic and alkaline media at OCP as well as in the passive state.

Experimental procedure

The austenitic stainless steel specimens chosen for these studies were of type 316LN with the composition given in Table 1. The solution-annealed specimens were cold worked up to 25% by rolling. The specimens of size 10×10 mm^2 were mounted in araldite and polished up to 1 μm finish. These specimens were cleaned with soap solution and dried. The specimens were cleaned cathodically at –1.0 with respect to a saturated calomel electrode (SCE) in deaerated 0.5 M H_2SO_4 containing 100 mg of NH_4SCN for 5 min and thereafter open circuit potential (OCP) was allowed to stabilize for 30 min. Potentiodynamic anodic polarization experiments were carried out on these specimens in the same solution at 1 mV/s scan rate. All the electrode potentials were measured against saturated calomel electrode (SCE). From these experiments a passive potential of +200 mV(SCE) was found to be suitable for conducting EIS studies during passivation. A freshly polished specimen was used for EIS studies, wherein, an initial 30 min time was allowed to lapse for the stabilization of the electrode potential, before the initiation of EIS experiment at OCP. After the EIS experiment at OCP, the specimen was anodically polarized up to +200 mV(SCE) at 1 mV/s scan rate and thereafter the potential of +200 mV(SCE) was potentiostatically impressed upon it for 10 min. At the end of this period, EIS experiment was conducted at the same impressed potential. EIS experiment was conducted using a sinusoidal AC signal of 10 mV in a frequency range of 10^5 to 10^{-2} Hz. All the above experiments were also carried out using freshly polished specimens in deaerated 1 M $NaHCO_3$ solution (pH = 8). However, the passivation potential for EIS studies was chosen to be +500 mV(SCE), all other experimental parameters remaining constant.

Table 1 Chemical composition of 316L(N) stainless steel, wt.%

Element	Indigenous (ASP) stainless steel
C	0.025
Cr	18.16
Ni	11.9
Mo	2.4
N	0.067
Mn	1.62
Si	0.28
P	0.044
S	0.010
Ti	0.019
Nb	0.032
Cu	0.560
Co	0.218
B	0.0017
W	<0.055
Sn	<0.004
Pb	<0.006
As	<0.006
Al	0.030
V	0.064

Results and discussion

Potentiodynamic anodic polarization diagrams for 316LN SS in deaerated acidic medium shown in Fig. 1a, exhibited a range of passivity approximately between 0.0 V(SCE) to 1.0 V(SCE), the passive currents observed being in the range of 20–50 μA/cm^2 for all the specimens. Since some specimens showed breakdown and repassivation above 0.6 V(SCE), EIS experiments were performed at 0.2 V(SCE). The potentiodynamic anodic polarization studies in deaerated alkaline medium showed (Fig. 1b, Table 2) a different pattern. Though, all the specimens showed complete passivation beyond OCP, the passive currents gradually increased until 0.4 V(SCE) and thereafter remained almost constant till they reached transpassive potential. Thus, the region of constant passive current at +0.5 V(SCE) was chosen to conduct EIS studies. In order to study the effect of cold work on the electrochemical parameters, critical anodic current density values (I_{cr}) and primary passivation potential values (E_{pp}) were determined in deaerated acidic solution. Similarly, passive current density values (I_{pas}) were determined in both the media at 0.2 V(SCE) and at 0.5 V(SCE) for acidic and alkaline media respectively. The I_{cr} values were found to increase continuously with increase in cold work (Fig. 2a), however, the change in the primary passivation potential values (E_{pp}) was not significant. Corrosion current density values (I_{corr}) were calculated using the Tafel fitting technique and plotted alongside the passive current

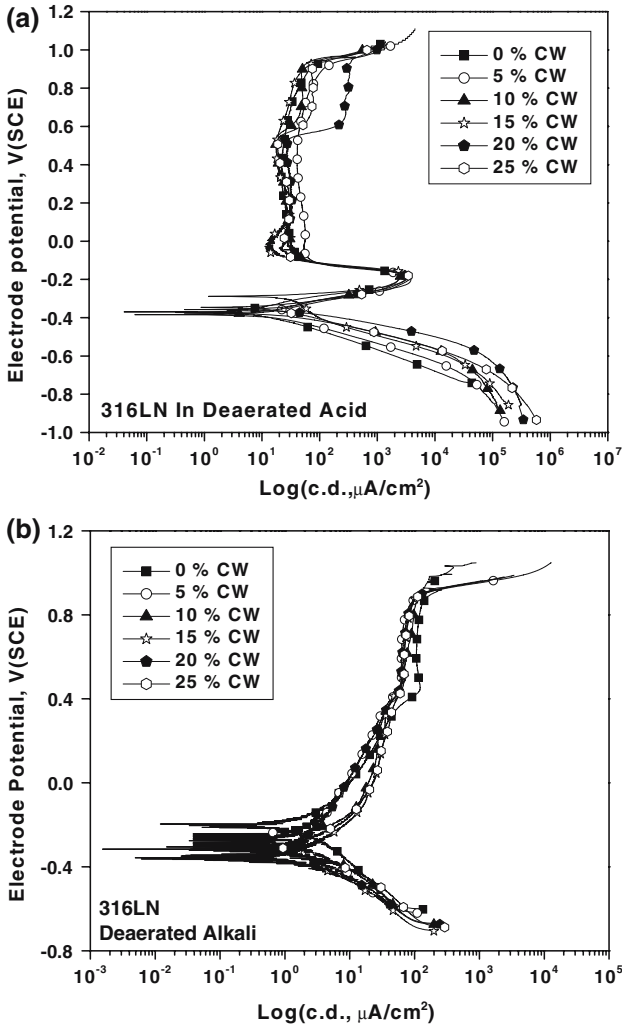

Fig. 1 Potentiodynamic anodic polarization curves for 316LN stainless steel in deaerated acidic (**a**) and deaerated alkaline media (**b**)

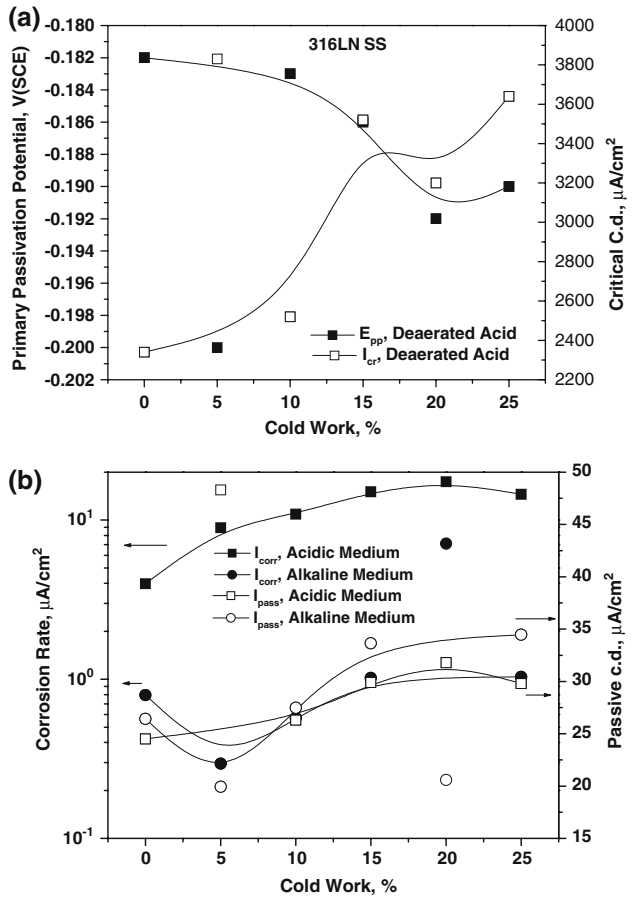

Fig. 2 Electrochemical parameters obtained from potentiodynamic polarization curves, (**a**) I_{cr}, E_{pp} in deaerated acidic medium, (**b**) I_{corr} I_{pas} in both media

density values (Fig. 2b). I_{corr} values were found to increase with increase in the cold work in acidic medium, however, similar trend was not observed in alkaline medium (Fig. 2b). Passive current density values too showed an increase with increase in cold work in both the media (Fig. 2b). Impedance values and phase angle values were plotted in the Bode plot format in order to distinguish clearly the resistive and capacitive regions. Impedance values (|Z|) at $f \rightarrow 0$ (where f is the frequency in Hz), give the $R_p + R_{sol}$ values, where R_p is the polarization resistance across the metal/solution interface and Rsol, is the solution resistance. Impedance values obtained at OCP and after passivation at +0.2 V(SCE) in deaerated acidic solution showed an increase in the $R_p + R_{sol}$ by almost one order of magnitude, indicating a higher value of R_p due to passivation (Fig. 3a, b). On the other hand, in deaerated alkaline solution, $R_p + R_{sol}$ values were found to be higher at OCP than after passivation at +0.5 V(SCE) (Fig. 3c, d). The phase angle plots suggest the nature of the film and its protectiveness, qualitatively. A broader capacitive loop indicates better film formation. The capacitive loops observed in deaerated acidic solution at OCP showed only a single time-constant, however after passivation the capacitive loops broadened for all the cold-worked

Table 2 Values of the ratio of *a*/*b* for 316LN in different media

Cold Work, %	Deaerated Acidic solution		Deaerated Alkaline Solution	
	At OCP	After Passivation	At OCP	After Passivation
0	9.3	21.9	17.3	19.5
5	10.8	16.4	12.2	8.7
10	9.8	10.3	11.4	10.0
15	7.6	10.5	6.3	11.8
20	7.6	10.3	12.5	7.4
25	10.2	8.7	7.1	7.7

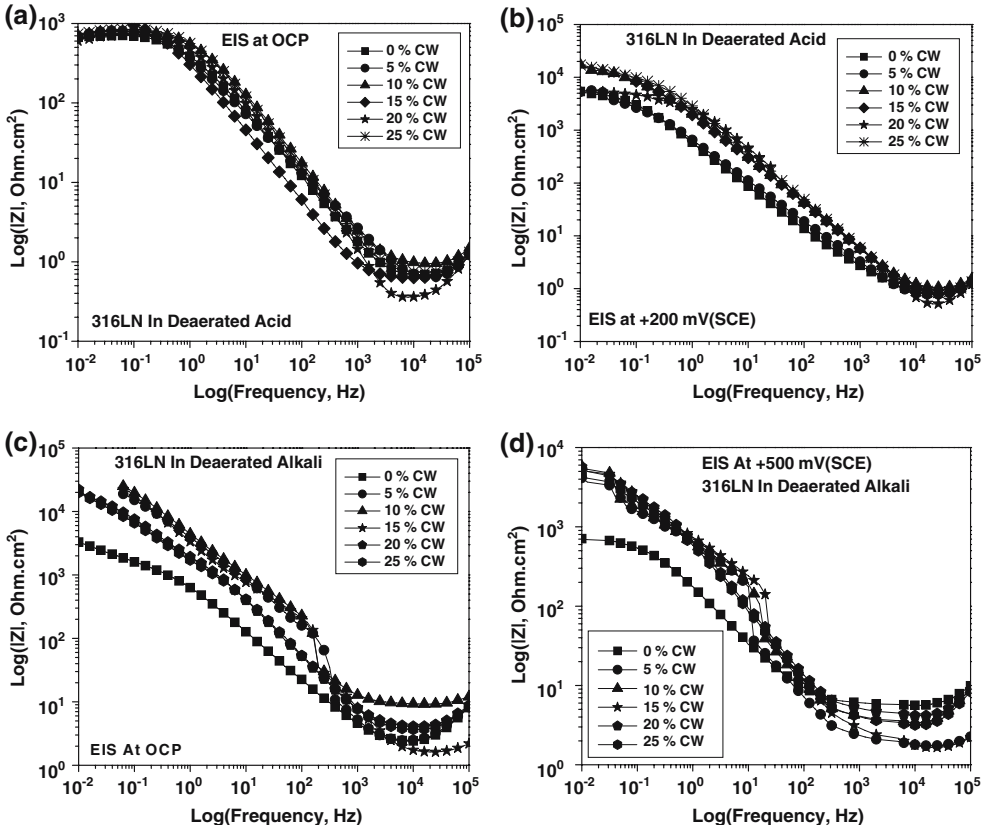

Fig. 3 Impedance plots for 316LN stainless steel in deaerated acidic medium (**a**) at OCP, (**b**) at +200 mV(SCE) and in deaerated alkaline medium (**c**) at OCP and (**d**) at +500 mV(SCE)

specimens (Fig. 4a, b). In deaerated alkaline solution, the phase angle plots showed two time-constants at OCP (except for 0% CW) but only a single time-constant after passivation (Fig. 4c, d). A phenomenon of this nature could be explained by using a bilayer model of the passive film on the surface, where the outer layer is porous. The pores in the outer layer which formed at OCP were sealed during passivation process, thus increasing the film stability further, resulting in the single time-constant [14, 15]. Nyquist plots (Fig. 5a, b) showed the typical depressed semi-circles in deaerated acidic solution both at OCP and after passivation, suggesting that the, hydrogen evolution reaction in both cases was under charge-transfer control [1]. The other Nyquist plots showed the typical charge-transfer-dominated region with some diffusion control (Fig. 5b–d). The shapes of such Nyquist plots (Fig. 5b–d) were earlier observed by Epelboin et al. [16]. for nickel and chromium in sulphuric acid solution, and by Armstrong and Edomondson [17]. for chromium in sulphuric acid solution. This behaviour was interpreted as due to the film formation coupled with the restricted diffusion process [18]. The Rp values and the capacitance values were obtained both by Nyquist and Bode fits and were plotted as a function of cold work (Fig. 6a–d). Increase in R_p values after passivation in acidic medium was noticeable (Fig. 6a) compared to the decrease of the same after passivation in alkaline medium (Fig. 6c). R_p values showed an increase with increase in cold work in acidic medium after passivation whereas this trend was reversed in alkaline medium (Fig. 6a, c). Capacitance values were found to decrease continuously with increase in cold work in both the media at OCP as well as after passivation, though the sharp decrease was noticed in acidic medium after passivation and in alkaline medium at OCP (Fig. 6b, d). Capacitance of the film/solution interface is directly related to the film thickness as,

$$C = \frac{\varepsilon \varepsilon_0 A}{d} \tag{1}$$

where, ε is the dielectric constant of the oxide film, ε_o is the permittivity of the space and A is the electrode area and d is the film thickness. Here it was assumed that the surface film is homogeneous in its dielectric properties with a dielectric constant of 15.6. The value of 15.6 for the dielectric constant was obtained for the films formed on AISI 304 in 0.5 M H_2SO_4 [19] and used by others [20]. Thus, it was inferred that, in the acidic solution, the passive film thickened significantly

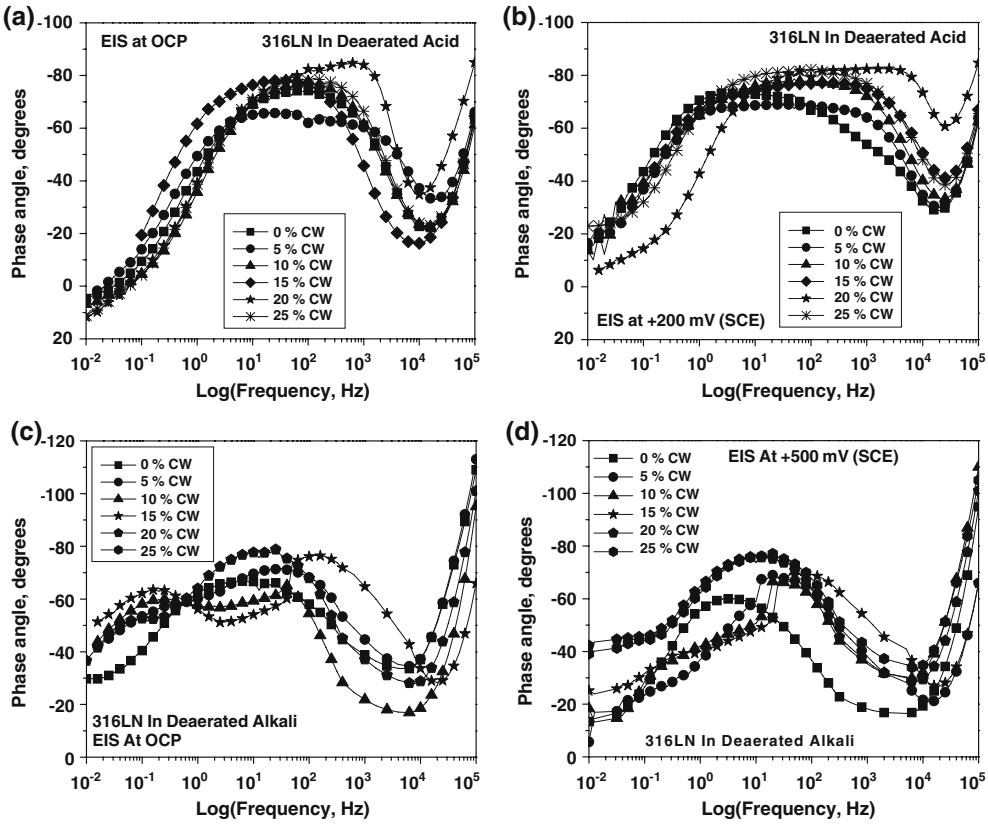

Fig. 4 Phase angle plots for 316LN stainless steel in deaerated acidic medium (**a**) at OCP, (**b**) at +200 mV(SCE) and in deaerated alkaline medium (**c**) at OCP and (**d**) at +500 mV(SCE)

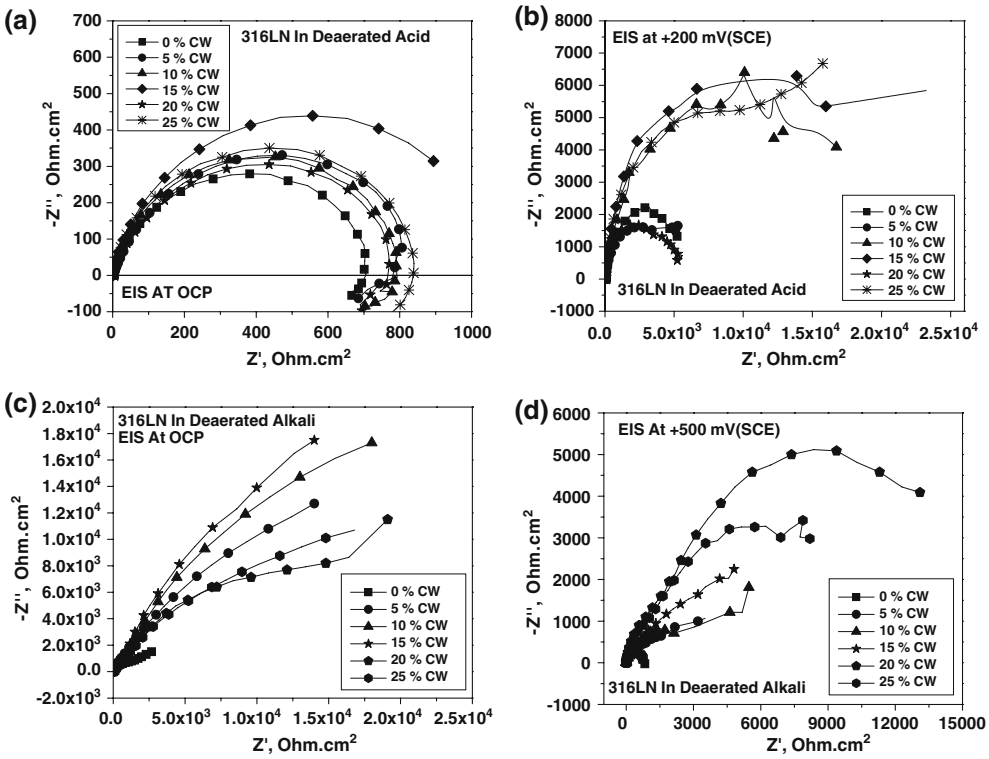

Fig. 5 Nyquist plots for 316LN stainless steel in deaerated acidic medium (**a**) at OCP, (**b**) at +200 mV(SCE) and in deaerated alkaline medium (**c**) at OCP and (**d**) at +500 mV(SCE)

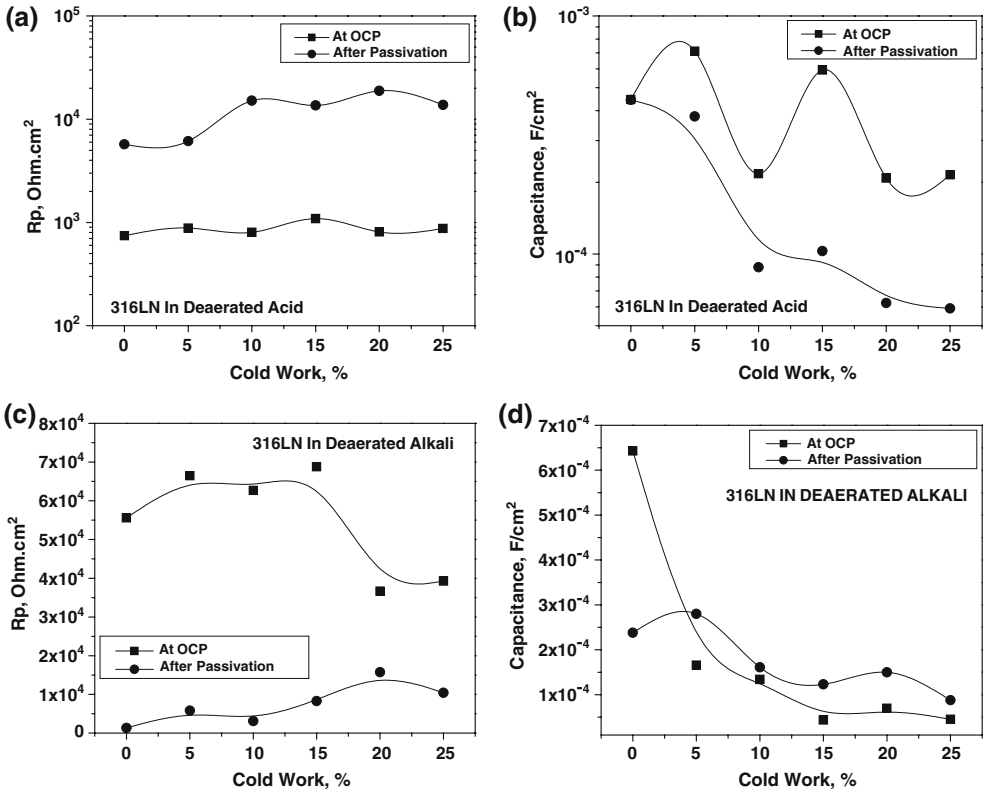

Fig. 6 Plots showing variation of Rp values and capacitance in deaerated acidic medium (**a**, **b**) and in deaerated alkaline medium (**c**, **d**) at OCP and after passivation for 316LN stainless steel as a function of cold work

as a function of cold work after passivation. The same phenomenon was observed in alkaline medium at OCP.

From the relationship given in equation 1, film thickness was calculated using the capacitance values obtained by Bode and Nyquist fits (Fig. 7a). In acidic medium, the film thickness at OCP showed increase with increase in cold work, although this increase was more prominent above 5% cold work (Fig. 7a). A clear increase in the film thickness as a function of cold work was observed in acidic medium after passivation using both Nyquist and Bode capacitance values (Fig. 7b). Ferreira and Dawson showed [20] that, the capacitance of 316 stainless steel continuously decreased in a potential range of 200–600 mV(SCE) in 0.5 M H_2SO_4 and contended that the passive film formed in this potential range thickened continuously. Film thickness values in alkaline solution were almost similar at OCP (Fig. 7c, d) and after passivation for a given type of fit. The film thickness values obtained by using capacitance values from the Nyquist fits (0.1–0.4 Å) showed similarity with the values quoted in the literature [21–23]. Brox and Olefjord [21] obtained the thickness of the passive film for single-phase austenite as 0.34 Å in a solution with pH 9.3 based on the model developed for XPS data. It is reported [24] that the film thickness on 316 stainless steel was around 0.4 Å in borate buffer irrespective of the film-formation potential. Perhaps, the thickness values of the films observed in alkaline media were much similar at OCP and after passivation at 0.5 V(SCE).

Earlier [25] a bilayer model of passive films was suggested to describe the electronic properties accurately, wherein a p-type inner region of chromium oxide (near the metallic substrate) and an outer *n*-type layer of iron oxide and hydroxide (near the solution) formed. Subsequently, AES results supporting this model were published [24]. The equivalent parallel capacitance values of the film formed at OCP and during passivation were measured as a function of frequency. Usually capacitance measurements show hysteresis as, they were dependent on the direction of polarization (cathodic or anodic). Capacitance values depended on the frequency as well as on the pH. Figure 8(a, b) showed the frequency dependence of capacitance at OCP and at +0.2 V(SCE) in deaerated acidic solution. The much rapid decrease in the capacitance values showed by some of the specimens was attributed by Stimming [26] to a contribution of surface states created by OH^- adsorbed at the oxide surface. A similar frequency dependence of the capacitance was noticed by Engell and Ilschner [27] for passive iron in 1 N H_2SO_4. Ion movement in the semiconductors cause frequency effects, especially in

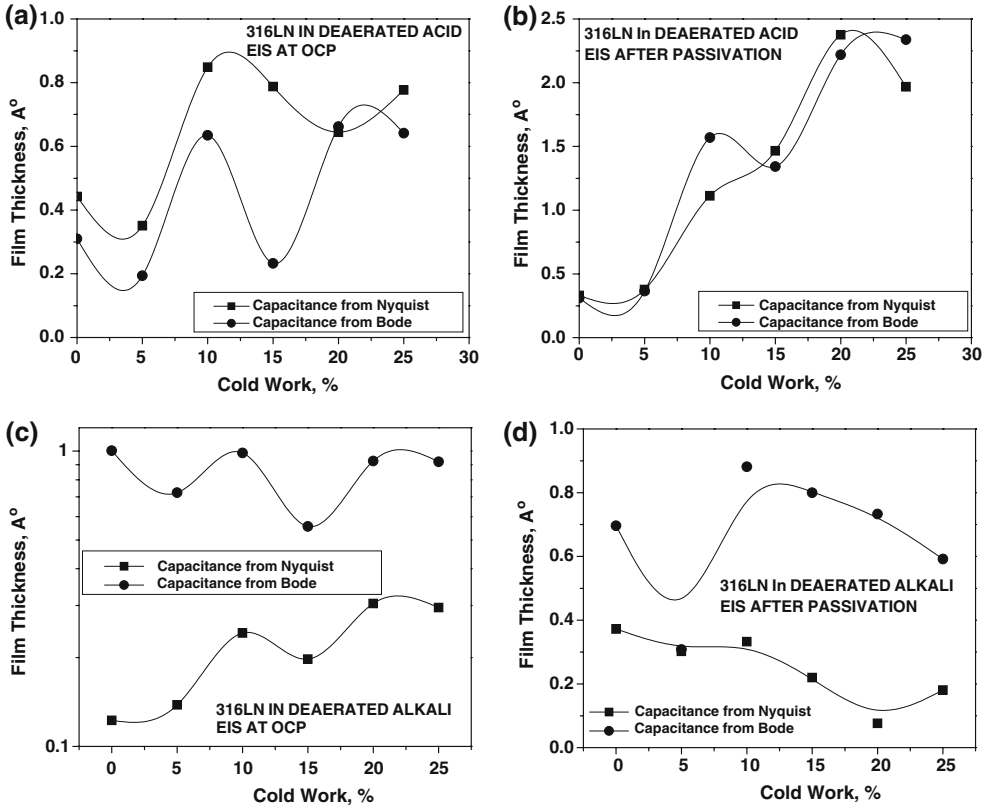

Fig. 7 Film thickness as a function of cold work for 316LN stainless steel in deaerated acidic solution (**a**, **b**) and in deaerated alkaline solution (**c**, **d**)

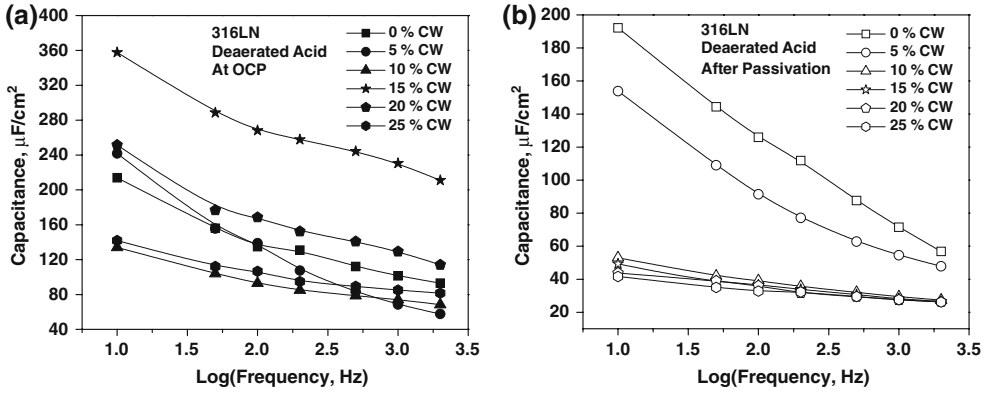

Fig. 8 Frequency dependence of capacitance values for 316LN ss in deaerated acidic solution at OCP (**a**) and at +0.2 V (SCE) (**b**)

heavily doped materials where the space charge region is very thin and the passive films generally satisfy these requirements. Similar plots of parallel capacitance against log f were also obtained in deaerated alkaline solution, however only representative plots are shown.

Figure 9 shows the variation of reciprocal capacitance values with log f at OCP and after passivation in both the media. It was noted that most of the plots showed a linear relation with log f, which is in accordance with the previous findings. In the work reported earlier, some of these plots at relatively more active potentials showed a bend towards the higher frequencies, a pattern observed in our studies at some of the plots at OCP.

Resistance measurements showed a strong dependence on the frequency. As shown in Fig. 10(a, b), resistance values directly varied with $1/f$ in both acidic and alkaline solutions at OCP and after passivation. It was earlier observed that [28], the linear relationship between resistance and $1/f$ held good in the same potential range in which 1/C and log$f$ showed a linear relationship, indicating that, these two parameters were dependent on each other.

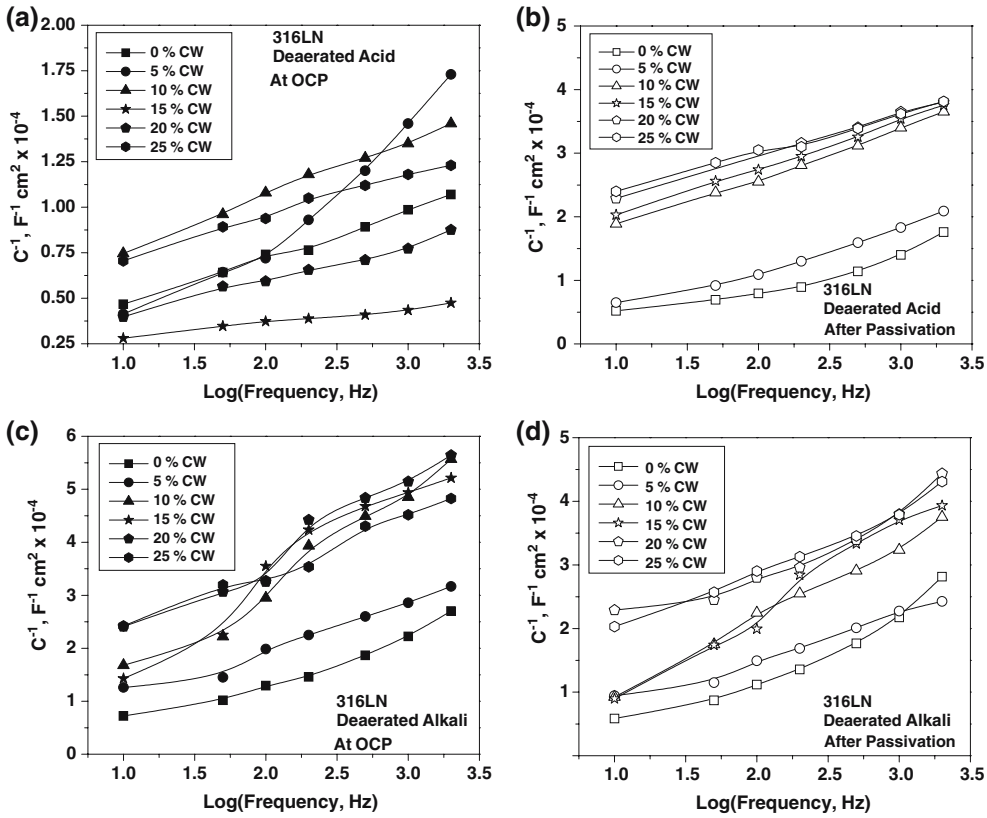

Fig. 9 Reciprocal capacitance against log f in deaerated acidic solution at OCP (**a**) and after passivation (**b**); in deaerated alkaline solution at OCP (**c**) and after passivation (**d**)

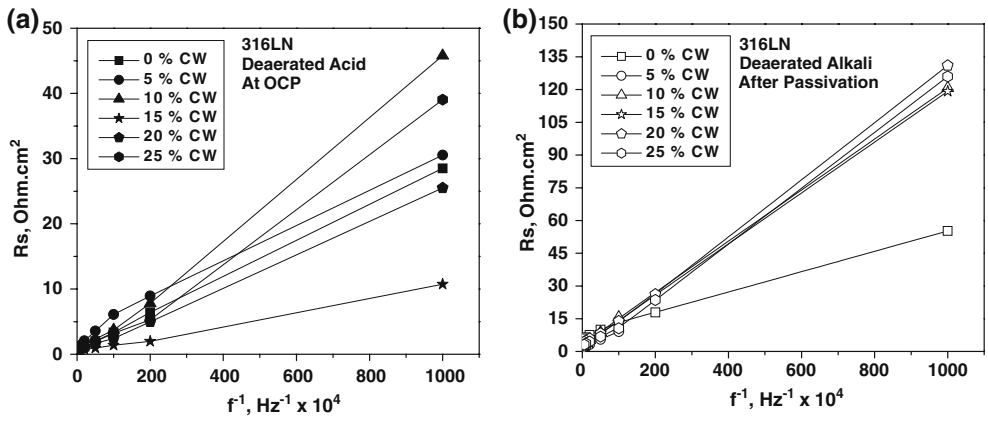

Fig. 10 Variation of the resistance with reciprocal frequency in deaerated acidic solution at OCP (**a**) and in deaerated alkaline solution after passivation (**b**) for 316LN ss

Analysis of the data on the passive films on niobium [29], tin [5] and various other semiconductors showed the following relationships between the frequency and the equivalent series capacitance (C_s) and series resistance (R_s), at constant potential.

$$\frac{1}{C_s} = \frac{1}{C_0} + a \log f \tag{2}$$

$$\frac{1}{R_s} = R_0 + \frac{b}{f} \tag{3}$$

where C_0, R_0, a and b are constants. Young [29] on the studies on passive niobium explained the results based on the above relationships. A numerical relationship was found out to be,

$$\frac{a}{b} = 9.2 \tag{4}$$

The above series of equations were found to be valid for our studies also, though the values of a/b were not exactly equal to 9.2 as found by Young [29] earlier. Some of the values were off the mark of 9.2,

Table 3 Transfer Coefficients and their ratios for 316LN stainless steel

Cold Work, %	Deaerated Acidic solution			Deaerated Alkaline Solution		
	α_a	α_c	α_a/α_c	α_a	α_c	α_a/α_c
0	0.436	0.477	0.91	0.205	0.236	0.87
5	0.471	0.479	0.98	0.223	0.307	0.73
10	0.416	0.696	0.60	0.301	0.286	1.05
15	1.169	0.653	1.79	0.189	0.305	0.62
20	0.483	0.743	0.65	0.150	0.259	0.58
25	0.685	0.664	1.03	0.217	0.341	0.64

but most of the values were found to be in a range of 7–10. In literature, other workers have reported values of *a*/*b* that differ from usual 9.2. The passive film on titanium [30] was found to show different values of *a*/*b*. It was contended [30] that the passive films on titanium did not represent an ideal dielectric, but are electrically inhomogeneous. The passive films on 316LN stainless steel used in our studies, perhaps too have inhomogeneous nature. However, the films formed on this stainless steel followed all the relationships shown above, that are normally followed by semiconductors.

It is reported by other workers that the passive films formed on stainless steels behave like *n*-type semiconductors in agreement with the results obtained for passive iron [10, 31]. Recently, Di Quarto et al. [32] contended that passive films were amorphous or strongly disordered semiconductors, which was usually supported by the impedance behaviour of these films at different frequencies. It was also noticed that, the Mott–Schottky plots (where capacitance, C^{-2} is plotted against the applied potential) obtained for 254 SMO, AISI 304 and ITM 40 stainless steels in acidic, alkaline and near-neutral media, showed positive slopes confirming that the films formed on these alloys were *n*-type semiconductors [28]. The photoelectrochemical measurements also indicate that the passive films are *n*-type semiconductors [33]. Hakiki et al. [24] showed that the passive films on AISI type 304 and 316 essentially showed *n*-type of semiconducting behaviour by using Mott–Schottky technique. According to the views published [24] the Mott–Schottky plots for 316 stainless steel showed a positive slope indicating *n*-type of semiconducting behaviour. Manning and Duquette [34] showed that the nature of the films on stainless steels could be studied using the anodic and cathodic transfer coefficients, α_a and α_c. The transfer coefficients are obtained as, $\alpha = 2.3\,RT/\beta nF$ where, β is the Tafel constant. Gerischer [35] explained that the ratio of the apparent anodic and cathodic transfer coefficients (α_a/α_c) determined the conductivity type; an oxide film is a p-type semiconductor when $\alpha_a/\alpha_c > 1$, and an *n*-type semiconductor when $\alpha_a/\alpha_c < 1$. In our studies, the transfer coefficients were calculated using the parameters from the anodic polarization data. It was observed that, except for two values, all the values of α_a/α_c were less than 1 (Table 3), showing that the passive films formed on 316LN stainless steels with different cold work were semiconductors of *n*-type.

Conclusions

From the corrosion and EIS studies on the AISI type 316LN stainless steel with 0–25% cold work in both deaerated acidic and alkaline media following conclusions were drawn:

1. EIS studies showed improvement in the passive film characteristics after passivation in acidic medium (increase of Rp and decrease of Capacitance), however, this trend was found to be reversed in alkaline medium (decrease of Rp and slight increase in Capacitance).
2. Two time constants observed in the phase angle plots at OCP and their subsequent disappearance after passivation in alkaline media, was attributed to the sealing of the double-layered porous film present at OCP.
3. Corrosion rates in acidic medium were found to increase with increase in cold work, however, no such trend was observed in the alkaline medium. The corrosion rates observed in alkaline medium were very low.
4. Semiconducting behaviour of the passive films at OCP and after passivation was established by using the series capacitance and resistance relationships and their slopes. It was established from the ratio of the transfer coefficients (α_a/α_c) that, the films formed on 316LN stainless steel were of *n*-type in nature irrespective of the amount of cold work.

Acknowledgement The authors thank Dr. H.S. Khatak, Head, CSTD for his constant encouragement during the process of above investigation. The assistance of Smt. K. Parimala in preparing the specimens is gratefully acknowledged.

References

1. Drogowska M, Menard H, Lasia A, Brossard L (1996) J Appl Electrochem 26:1169
2. Bianchi G, Cerquetti A, Mazza F, Torchio S (1972) Corr Sci 12:495
3. Young L (1961) Anodic oxide films. Academic Press, New York

4. Sunseri C, Piazza S, Di Paola A, Di Quarto F (1987) J Electrochem Soc 134:2410
5. Kapusta S, Hackerman N (1980) Electrochimica Acta 25:949
6. Ord JL, Bartlett JH (1965) J Eletrochem Soc 112:160
7. Cahan BD, Chen CT (1982) J Electrochem Soc 129:474
8. Wilhelm SM, Yun KS, Ballenger LW, Hackermann N (1979) J Electrochem Soc 126:419
9. Wheeler D, Cahan BD, Chen CT, Yeager EB (1978) In: Frankenthal RF, Kruger J (eds) Passivity of metals. The Electrochemical Society, New Jersey, 546 pp
10. Abrantes LM, Peter LM (1983) J Electroanal Chem 150:593
11. Okamoto G, Shibata T (1970) Corros Sci 10:371
12. Okamoto G (1973) Corros Sci 13:471
13. Ferreira MGS, Dawson JL (1985) J Electrochem Soc 132:760
14. Schmidt AM, Azambuja DS (2003) Mat Res 6:239
15. Pan J, Thierry D, Leygraf C (1996) Electrochim Acta 41:1143
16. Epelboin I, Keddam M, Morel P (1969) Proc. 3rd Int. Cong. on Metallic Corrosion, Moscow, USSR, 1966, Swets and Zeitlinger, Amsterdam, Holland, vol. 1, 110–118
17. Armstrong RD, Edomondson K (1973) Electrochim Acta 18:937
18. Jibara SM (1981) Ph. D. Thesis, UMIST, Manchester, England
19. Curley-Florino ME, Schmid GM (1980) Corro Sci 20:313
20. Ferreira MGS, Dawson JL (1985) J Electrochem Soc 132:760
21. Brox B, Olefjord I, Proc. Stainless Steel, 1984, Chalmers University of Technology; Goteborg; Sweden; 3–4 Sept. 1984, The Institute of Metals, London, UK, 1985, 134–143
22. Dobbelaar JAL, Herman ECM, De Wit JH (1992) Corros Sci 33:779
23. Gojic M, Marijan D, Kosec L (2000) Corrosion 56:839
24. Hakiki NE, Da Cunha Belo M, Simoes AMP, Ferreira MGS (1998) J Electrochem Soc 145:3821
25. Hakiki NE, Boudin S, Rondot B, Da Cunha Belo M (1995) Corros Sci 37:1809
26. Stimming U (1983) In: Froment M (ed) Passivity of metals and semiconductor. Elsevier, Amsterdam, 477 pp
27. Engell HJ, Ilschner B (1955) Z Elektrochem 59:716
28. Di Paola A (1989) Electrochimica Acta 34:203
29. Young L (1955) Trans Faraday Soc 51:1250
30. Gad Allah AG, Mazhar AA, E-Basiouny MS (1986) Corrosion 42:740
31. Azumi K, Ohtsuka T, Sato N (1987) J Electrochem Soc 134:1352
32. Di Quarto F, Sunseri C, Piazza S (1986) Ber Bunsenges Phys Chem 90:549
33. Di Paola A, Di Quarto F, Sunseri C (1986) Corros Sci 26:935
34. Manning PE, Duquette DJ (1980) Corros Sci 20:597
35. Gerischer H (1970) In: H Eyring (ed) Physical chemistry, An advanced treatise, vol. IXA. Academic Press, New York, 463 pp